Accepted Preprint first posted on 22 December 2017 as Manuscript JME-17-0260

SP600125 Suppresses *Keap1* Expression and Results in NRF2-mediated Prevention of Diabetic Nephropathy

Huan Zhang [1], Xiuxia Liu [2], Shanshan Zhou [3], Ye Jia [4], Ying Li [5], Yuguo Song [6, 7], Junnan Wang [8, *], Hao Wu [9, 10, †]

1. Operating theater, China-Japan Union Hospital of Jilin University, 126 Xiantai St., Changchun, Jilin, 130033, People's Republic of China

2. Department of Clinical Laboratory, The Second Hospital of Jilin University, 218 Ziqiang St., Changchun, Jilin, 130041, People's Republic of China, +86 15104486039

3. Cardiovascular Center, The First Hospital of Jilin University, 71 Xinmin St., Changchun, Jilin, 130021, People's Republic of China

4. Department of Nephrology, The First Hospital of Jilin University, 71 Xinmin St., Changchun, Jilin, 130021, People's Republic of China

5. Department of Dermatology, Affiliated Hospital of Beihua University, 12 Jiefang Rd., Jilin, Jilin, 132000, People's Republic of China

6. Research Institute of Clinical Immunology, Affiliated Hospital of Beihua University, 12 Jiefang Rd., Jilin, Jilin, 132000, People's Republic of China.

7. Research Center for Life Sciences, Beihua University, 3999 Binjiangdong Rd., Jilin, Jilin, 132013, People's Republic of China

8. Department of Cardiology, The Second Hospital of Jilin University, 218 Ziqiang St., Changchun, Jilin, 130041, People's Republic of China

9. Department of Nephrology, The Second Hospital of Jilin University, 218 Ziqiang St., Changchun, Jilin, 130041, People's Republic of China

10. The '973' National Basic Research Program of China, Changchun University of Chinese Medicine, 1035 Boshuo Rd., Changchun, Jilin, 130117, People's Republic of China

Running Head: JNK inhibition activates NRF2

Word Count: 4641

† Corresponding author who handles the manuscript:

Hao Wu

Department of Nephrology, The Second Hospital of Jilin University, 218 Ziqiang St., Changchun, Jilin, 130041, People's Republic of China;

The '973' National Basic Research Program of China, Changchun University of Chinese Medicine, 1035 Boshuo Rd., Changchun, Jilin, 130117, People's Republic of China

Email: wuhaobaha@jlu.edu.cn

Phone: +86 17390062119

* Corresponding author:

Junnan Wang

Department of Cardiology, The Second Hospital of Jilin University, 218 Ziqiang St., Changchun, Jilin, 130041, People's Republic of China

Email: jdeywjn@163.com

Phone: +86 13756536975

Abstract

c-Jun N-terminal kinase (JNK) contributes to the pathogenesis of diabetic nephropathy (DN). The JNK inhibitor SP600125 was reported to ameliorate DN. However, the mechanism remained unclear. We previously reported that SP600125 activated nuclear factor erythroid 2-related factor 2 (NRF2), a governor of the cellular antioxidant defense system, in the aortas of the diabetic mice. Given the critical role of NRF2 in preventing DN, the present study aimed to test whether or not NRF2 is required for SP600125's protection against DN. To test the role of NRF2 in SP600125's effect, streptozotocin-induced C57BL/6 wild type (WT) and *Nrf2* knockout (KO) diabetic mice were treated in the presence or absence of SP600125, for 24 weeks. To explore the mechanism by which SP600125 activates NRF2, mouse mesangial cells (MMCs) were treated with high glucose (HG), in the presence or absence of either SP600125 or JNK siRNA. SP600125 significantly attenuated the diabetes-induced renal oxidative stress, inflammation, fibrosis, pathological change and dysfunction in the WT, but not the *Nrf2* KO, mice. SP600125 inactivated JNK, inhibited kelch-like ECH-associated protein 1 expression, preserved NRF2 protein and facilitated its nuclear translocation in the kidneys of the WT mice, the effects of which were similarly produced by either SP600125 or JNK siRNA in HG-treated MMCs. Further, both SP600125 and JNK siRNA alleviated HG-induced mesangial oxidative stress, and expression of inflammatory and fibrotic genes. The present study demonstrates that NRF2 is required for SP600125's protection against DN. SP600125 activates NRF2 possibly via inhibition of JNK-induced *Keap1* expression.

Key Words: antioxidant; diabetic nephropathy; KEAP1; JNK; NRF2

1. Introduction

Diabetic nephropathy (DN) is the main cause of end stage renal disease (Dronavalli, et al. 2008), and to date, has not been effectively treated. Therefore, it is essential to discover novel targets and develop more effective medicines to prevent the development of DN.

c-Jun N-terminal kinase (JNK) belongs to the mitogen-activated protein kinases (MAPK) family and regulates the transcription activity of activator protein 1 (AP-1) by phosphorylation of c-Jun (Davis 2000). AP-1 activates the transcription of a cohort of genes, such as transforming growth factor beta 1 (*Tgf-β1*) (Weigert, et al. 2000) and fibronectin (*Fn*) (Lan, et al. 2013), which play important roles in the initiation and progression of DN (Schena and Gesualdo 2005). Enhanced JNK activity was observed in high glucose (HG)-treated mesangial cells (Gao, et al. 2016; Zhou, et al. 2014), in kidneys of diabetic mice (Gao et al. 2016; Pan, et al. 2013; Wang, et al. 2015) and in kidney biopsy tissue from patients with DN (De Borst, et al. 2007). Therefore, targeting JNK could be a promising strategy in prevention of DN. SP600125 is a specific inhibitor of JNK (Bogoyevitch, et al. 2004). Previous studies reported the beneficial effect of SP600125 on DN (Gao et al. 2016; Hong, et al. 2016; Wang et al. 2015). Despite the finding of decreased expression of several pro-fibrotic and pro-inflammatory genes, the mechanism through which SP600125 ameliorated DN was unclear.

Nuclear factor erythroid 2-related factor 2 (NRF2) is a master regulator of cellular antioxidant defensive activity (Zheng, et al. 2011). As a transcription factor, NRF2 turns on the transcription of various antioxidant genes, such as heme oxygenase 1 (*Ho1*) and NAD(P)H dehydrogenase (quinone) 1 (*Nqo1*), leading to the increased

antioxidants which function as scavengers for diabetes-induced free radicals (Ruiz, et al. 2013). Accumulating evidence has demonstrated the pivotal role of NRF2 in self-defense against the pathogenesis of DN, since the *Nrf2* gene knockout (KO) mice developed more severe nephropathy under diabetic condition, as compared with the wild type (WT) mice (Jiang, et al. 2010; Wu, et al. 2015; Wu, et al. 2016). In our previous study, SP600125 was found to activate NRF2 in the aortas of the diabetic mice (Liu, et al. 2014), suggesting that JNK may negatively regulate NRF2. However, whether or to what extent NRF2 is required for SP600125's protective effect was unknown. By using *Nrf2* KO mice, the present study aimed to explore the role of NRF2 in SP600125's protection against DN.

Kelch-like ECH-associated protein 1 (KEAP1) is a key negative regulator of NRF2 (Kensler, et al. 2007). KEAP1 sequesters NRF2 in cytoplasm, restricting NRF2 from nuclear translocation and promoting its proteasomal degradation (Zhang and Hannink 2003). JNK might be an upstream regulator of KEAP1, since 36 c-Jun binding sites were found between -3000bp to -1bp within the promoter region of the mouse *Keap1* gene (Jaspar Database). Thus, JNK might inhibit NRF2 through induction of *Keap1* expression. By determining the renal level of *Nrf2* mRNA, the preservation of NRF2 protein, the proportion of the NRF2 nuclear translocation, and the expression of *Keap1*, the present study tested the actions of SP600125 in regulation of NRF2. To further verify the effect of JNK inhibition on NRF2 signaling and HG-induced injury, SP600125 was studied in HG-treated mouse mesangial cells (MMCs), by comparing to the effect of JNK siRNA.

In summary, the present study aimed to answer the following questions: (1) whether or not SP600125 activates NRF2 in DN; (2) whether or to what extent NRF2

is required for SP600125's protection against DN; (3) how does SP600125 activate NRF2.

2. Materials and methods

2.1 Animal treatment

C57BL/6 WT (*Nrf2*+/+) and *Nrf2* KO (*Nrf2*-/-) mice were obtained through breeding of heterozygotes (*Nrf2*+/-) (Dong, et al. 2017; Zheng et al. 2011). All mice were housed in the Animal Center of Jilin University at 22 ℃, on a 12:12-hour light-dark cycle with free access to rodent feed and tap water. The Institutional Animal Care and Use Committee at Jilin University approved all experimental procedures for these animals.

Eight-week-old male mice received either sodium citrate or streptozotocin (STZ, 50 mg/kg daily, dissolved in 0.1 M sodium citrate, pH 4.5; Sigma-Aldrich, Shanghai, PRC) through intraperitoneal injection for 5 consecutive days. One week after the last injection of STZ, fasting glucose levels (4-hour fast) were measured. Mice with a fasting glucose level above 13.89 mM were considered diabetic. Diabetic and age-matched control mice were then given by gavage with SP600125 (5 mg/kg, dissolved in 1% CMC-Na solution; Medchem Express, Shanghai, PRC) or 1% CMC-Na solution, once every 2 days (Pan, et al. 2014), for 24 weeks.

Blood glucose was recorded on days 0, 28, 56, 84, 112, 140 and 168 post diabetes onset. Urinary albumin and creatinine were recorded on day 168 post diabetes onset. The mice were then killed and their kidneys harvested for analysis.

2.2 Analysis of kidney dysfunction

A mouse albumin kit (Bethyl Laboratories, Montgomery, TX) and a QuantiChrom™ Creatinine Assay Kit (BioAssay Systems, Hayward, CA) were used to determine urinary albumin and creatinine on spot urine samples following the manufacturer's instructions. Urinary albumin to creatinine ratio (UACR) was calculated to reflect kidney dysfunction.

2.3 Morphological analysis

After harvesting, the kidney tissues were fixed immediately in 10% buffered formalin solution and were embedded in paraffin and sectioned into 5-μm-thick sections onto glass slides. The sections were processed for Periodic acid-Schiff (PAS) and Masson's trichrome staining. Morphometric analysis was quantified using Image-Pro Plus 6.0 software (Media Cybernetics Inc, Bethesda, MD). Selection of areas to photograph and scoring was done by people blind to the identity of the samples.

2.4 Immunohistocheminal (IHC) analysis

IHC staining was performed as previously described (Wu, et al. 2014a) to assess the status of renal oxidative damage and antioxidant activity, using primary antibodies against 3-nitrotyrosine (3-NT, Millipore, Temecula, CA, USA; 1:100), HO1 (Santa Cruz Biotechnology, 1:100) and NQO1 (Santa Cruz Biotechnology, 1:100).

2.5 Cell culture and experiments

MMCs were isolated and cultured as previously described (Sun, et al. 2017). Passages 5 to 7 were used for the experiments (Sun et al. 2017). To determine the

effect of SP600125 and JNK siRNA on JNK activity, *Keap1* expression, NRF2 signaling and HG-induced injury, MMCs were subjected to HG (25 mM), in the presence or absence of 10 μM SP600125 (Gao et al. 2016; Ho, et al. 2007; Zhou et al. 2014) or JNK siRNA (100 nM, GenePharma, Suzhou, Jiangsu, PRC), for 48 hours. The negative control siRNA was purchased from GenePharma. The transfection reagent RFect^{PM} was provided by Changzhou Bio-generating Biotechnologies, Changzhou, PRC.

2.6 Western blot analysis

Western blot analysis was performed using kidney cortex as previously described (Cai, et al. 2005). The primary antibodies were: anti-connective tissue growth factor (CTGF, Santa Cruz Biotechnology, Dallas, TX, USA, 1:500), anti-GAPDH (Santa Cruz Biotechnology, 1:3,000), anti-histone H3 (Santa Cruz Biotechnology, 1:1000), anti-HO1 (Santa Cruz Biotechnology, 1:1000), anti-inducible nitric oxide synthase (iNOS, Cell Signaling Technology, Beverly, MA, USA, 1:1000), anti-total cellular c-Jun (t-c-Jun, Cell Signaling Technology, 1:500), anti-total cellular JNK (t-JNK, Cell Signaling Technology, 1:1000), anti-KEAP1 (Santa Cruz Biotechnology, 1:500), anti-NQO1 (Santa Cruz Biotechnology, 1:1000), anti-NRF2 (Santa Cruz Biotechnology, 1:1000), anti-phosphorylated-c-Jun (p-c-Jun, Cell Signaling Technology, 1:500), anti-phosphorylated-JNK (p-JNK, Cell Signaling Technology, 1:500), anti-TGF-β1 (Cell Signaling Technology, 1:1000), anti-tumor necrosis factor alpha (TNF-α, Cell Signaling Technology, 1:500), and anti-vascular cell adhesion molecule 1 (VCAM-1, Santa Cruz Biotechnology, 1:1000).

193 **2.7 Real-time PCR**

194 Quantitative real-time PCR was performed as previously described (Wang, et al.
195 2009; Wu, et al. 2014b). Primers for collagen 4 (*Col4*), *Fn*, *Gapdh*, *Nqo1*,
196 intercellular adhesion molecule 1 (*Icam-1*), *Ho1*, *iNos*, *Keap1*, *Nrf2* and *Vcam-1* were
197 all purchased from Life Technologies (Shanghai, PRC).

198

199 **2.8 Quantitative analysis of lipid peroxides**

200 Renal malondialdehyde (MDA) concentration was calculated following the
201 instructions by a lipid peroxidation assay kit from Nanjing Jiancheng Bioengineering
202 Institute, Nanjing, Jiangsu, PRC.

203

204 **2.9 Isolation of nuclei**

205 Nuclei of renal tissue and MMCs were isolated using a nuclei isolation kit
206 (Sigma-Aldrich) as previously described (Dong et al. 2017; Sun et al. 2017),
207 following the manufacturer's instructions.

208

209 **2.10 Statistical analysis**

210 Eight mice per group were studied. The measurements for each group were
211 summarized as means ± SD. Image Quant 5.2 (GE Healthcare Bio-Sciences,
212 Pittsburgh, PA) was used to analyze Western blots. Two-way ANOVA was
213 performed for the comparisons among different groups of the two types of the mice.
214 One-way ANOVA was performed for comparisons among different groups of either
215 the WT or the *Nrf2* KO mice, as well as different groups of the cell experiments. Post
216 hoc pairwise comparisons were then performed using Tukey's test with Origin 8.6

data analysis and graphing software Lab (OriginLab, Northampton, MA, USA). A test is significant if $p < 0.05$.

3. Results

3.1 Deletion of the *Nrf2* gene led to a complete abolishment of SP600125's protection against diabetes-induced albuminuria and renal pathological change.

Blood glucose levels were monitored every four weeks post diabetes onset. Both the WT and the *Nrf2* KO diabetic mice had significantly increased blood glucose levels at all the time points, as compared with their respective controls (Fig. 1A). SP600125 did not alter blood glucose under both the diabetic and the non-diabetic conditions, in both types of the mice (Fig. 1A). No significant difference in blood glucose level was detected between the WT and the *Nrf2* KO mice, under both the diabetic and non-diabetic conditions (Fig. 1A). However, as compared with the WT diabetic mice, the *Nrf2* KO diabetic mice developed remarkably higher UACR (Fig. 1B) and more severe renal pathological change, as shown by PAS staining (Fig. 1C) and Masson's trichrome staining (Fig. 1D), including the more drastic increase in glomerular area (Fig. 1E), mesangial matrix (Fig. 1F) and Masson's positive area (Fig. 1G). These results confirmed the critical role of NRF2 in self-defense against DN. Notably, in the WT mice, SP600125 significantly attenuated the diabetes-induced elevation of UACR (Fig. 1B, left panel) and pathological change (Fig. 1E-G, left panels). However, these beneficial effects of SP600125 did not exist in the *Nrf2* KO mice (Fig. 1B, E, F, right panels), with an exception of the amelioration of renal fibrosis (Fig. 1G, right panel). Nonetheless, the efficacy of SP600125 in decreasing renal fibrosis was blunted in the absence of NRF2, since

SP600125 decreased renal fibrosis by 58.10 percent in the WT mice whereas only by 25.47 percent in the *Nrf2* KO mice (Fig. 1G). Therefore, NRF2 plays a major role in SP600125's protection against the diabetes-induced albuminuria and renal pathological change.

3.2 NRF2 was required for SP600125's alleviation of the diabetes-induced renal oxidative stress, inflammation and fibrosis.

Renal nitrosative damage was reflected by IHC staining of 3-NT (Fig. 2A), which showed a preferable expression of 3-NT in the glomeruli. Further, renal oxidative stress, inflammation and fibrosis were evaluated at the molecular level. The levels of the oxidative stress indicators MDA (Fig. 2B) and iNOS protein (Fig. 2C), the protein levels of the pro-inflammatory markers TNF-α (Fig. 2D) and VCAM-1 (Fig. 2E), and the protein levels of the pro-fibrotic parameters TGF-β1 (Fig. 2F) and CTGF (Fig. 2G) were measured in both types of the mice, all of which were elevated under the diabetic condition (Fig. 2B-G). SP600125 attenuated these indices in the WT, but not the *Nrf2* KO, diabetic mice (Fig. 2B-F), except for a mild decrease (26.74%) in CTGF in the *Nrf2* KO diabetic mice (Fig. 2G, right panel), in contrast to the WT mice (47.97%, Fig. 2G, left panel). These results indicate that NRF2 predominantly mediates SP600125's protection against diabetes-induced renal oxidative stress, inflammation and fibrosis.

3.3 SP600125 preserved renal NRF2 protein and facilitated NRF2 nuclear translocation and function, without altering *Nrf2* mRNA.

Renal *Nrf2* expression and function were evaluated in the following study. Neither *Nrf2* mRNA (Fig. 3A, right panel) nor NRF2 protein (Fig. 3B, right panel) were detectable in the kidneys of *Nrf2* KO mice, as a confirmation of the *Nrf2* gene deletion. SP600125 did not alter *Nrf2* mRNA in the WT mice (Fig. 3A, left panel). Rather, it increased total cellular NRF2 (t-NRF2, Fig. 3B, left panel) and nuclear NRF2 (n-NRF2, Fig. 3C, left panel) in both the WT diabetic and non-diabetic mice. These results suggest that SP600125 regulates *Nrf2* expression at the protein, but not the mRNA, level. NRF2 nuclear translocation was further evaluated by calculating the ratio of n-NRF2/histone H3 to t-NRF2/GAPDH, which was enhanced by SP600125 under both the diabetic and the non-diabetic conditions (Fig. 3D). Further, the mRNA levels of *Ho1* and *Nqo1* were both significantly increased by SP600125 in the WT, but not *Nrf2* KO, mice (Fig. 3E, F). It is noted that, compared to the WT mice, the *Nrf2* KO mice expressed less renal *Ho1* and *Nqo1* mRNAs under both the diabetic and non-diabetic conditions (Fig. 3E, F), a result in line with the renal susceptibility of the *Nrf2* KO mice upon diabetes (Fig. 1B-G). Renal expression of HO1 and NQO1 was further assessed by IHC staining, which showed an increase of these antioxidants by SP600125 in the glomeruli of the WT mice (Fig. 3G, H, upper panels). This effect did not exist in the glomeruli of the *Nrf2* KO mice (Fig. 3G, H, lower panels). Collectively, SP600125 was found to activate NRF2 signaling via preserving NRF2 protein and facilitating its nuclear translocation, rather than enhancing *Nrf2* transcription.

3.4 SP600125 decreased *Keap1* expression through inhibition of JNK activity.

Given that KEAP1 restricts NRF2 from nuclear translocation and promotes proteasomal degradation of NRF2 (Zhang and Hannink 2003), we speculated that the observed preservation and relocation of NRF2 by SP600125 might be due to a down-regulated KEAP1 expression or function. To test this hypothesis, renal *Keap1* expression was determined. As expected, SP600125 markedly decreased *Keap1* mRNA (Fig. 4A) and protein (Fig. 4B) in both types of the mice, under both the diabetic and the non-diabetic conditions. The inhibitory effect of SP600125 on JNK activity was further verified by the decreased phosphorylation of renal JNK (Fig. 4C) and c-Jun (Fig. 4D).

The following study was to further test whether inhibition of JNK activity could lead to a down-regulated *Keap1* expression. Thus, HG-treated MMCs were subjected to either SP600125 or JNK siRNA. MMC was selected for the study because of the diabetes-induced remarkable pathological change observed in Fig. 1C-G. SP600125 decreased the ratio of p-JNK to t-JNK (Fig. 4E, left panel), but not t-JNK to GAPDH (Fig. 6A, middle panel). On the contrary, the ratio of t-JNK to GAPDH, but not p-JNK to t-JNK, was drastically decreased by JNK siRNA (Fig. 4E, left and middle panels). Despite these distinct actions of SP600125 and JNK siRNA (Fig. 4E, left and middle panels), both of them led to a significant decrease in the ratio of p-JNK to GAPDH (Fig. 4E, right panel). Inactivation of JNK by SP600125 and JNK siRNA was further confirmed by the decreased phosphorylation of c-Jun (Fig. 4F). SP600125 and JNK siRNA also led to an inhibition of *Keap1* expression at both the mRNA (Fig. 4G) and the protein (Fig. 4G) levels, the result of which was in accordance with the findings *in vivo* (Fig. 4A, B).

Taken together, by comparing with the effect of JNK siRNA, SP600125 was found to inhibit *Keap1* expression via inactivation of JNK.

3.5 Both SP600125 and JNK siRNA preserved NRF2 protein and enhanced its nuclear translocation and function.

Given the verified JNK inactivation-induced inhibition of *Keap1* expression (Fig. 4G, H), the following study tested in HG-treated MMCs whether both SP600125 and JNK siRNA could preserve NRF2 protein and trigger its nuclear translocation. As shown in Fig. 5, both SP600125 and JNK siRNA increased t-NRF2 (Fig. 5A), n-NRF2 (Fig. 5B) and ratio of n-NRF2/histone H3 to t-NRF2/GAPDH (Fig. 5C). The two JNK inhibiting approaches further enhanced the mRNA levels of *Ho1* and *Nqo1* (Fig. 5D, E).

3.6 JNK inhibition by either SP600125 or JNK siRNA decreased oxidative damage and expression of inflammatory and fibrotic genes in HG-treated MMCs.

Finally, comparing to the effect of JNK siRNA, the role of JNK inhibition in the protective effect of SP600126 was tested by determining MDA levels (Fig. 6A) as well as mRNA expression of *iNos* (Fig. 6B), *Vcam-1* (Fig. 6C), *Icam-1* (Fig. 6D), *Fn* (Fig. 6E) and *Col4* (Fig. 6F) in HG-treated MMCs. All these parameters were significantly decreased by SP600125 or JNK siRNA (Fig. 6A-F). Hence, the benefits produced by SP600125 were mediated by JNK inactivation.

4. Discussion

The present study researched the action of SP600125 in *Nrf2* expression and function in the protection against DN. By using *Nrf2* KO mice, NRF2 was found to be the major factor through which SP600125 ameliorated DN. In the kidneys of the WT mice, SP600125 inactivated JNK, inhibited *Keap1* expression, preserved cellular NRF2 protein level and facilitated NRF2 nuclear translocation. By comparing to the effect of JNK siRNA, SP600125 was found to inhibit *Keap1* expression, activate NRF2 signaling and attenuate HG-induced deleterious effects in HG-treated MMCs via inactivation of JNK. The present study indicates a negative regulatory effect of JNK on NRF2 in DN possibly through JNK-induced *Keap1* expression and may thus provide JNK inhibition as a feasible strategy for prevention of DN.

By phosphorylating c-Jun and thereby activating AP-1(Davis 2000), JNK induces the transcription of *Tgf-β1* (Weigert et al. 2000) and *Fn* (Lan et al. 2013), both of which play key roles in the pathogenesis of DN (Schena and Gesualdo 2005). Inhibition of JNK by SP600125 decreased *Tgf-β1* (Gao et al. 2016) and *Fn* (Gao et al. 2016; Wang et al. 2015), and ameliorated DN. It was therefore speculated that JNK may contribute to the development of DN through activating *Tgf-β1* and *Fn*. In the present study, NRF2 was found to be another downstream target of JNK. Different from the positive impact on *Tgf-β1* and *Fn* gene transcription, JNK negatively regulated *Nrf2* expression at the protein, but not the mRNA, level (Fig. 3A, B). NRF2 played a major role in the protection by SP600125, since most of the beneficial effects of SP600125 did not exist in the absence of NRF2 (Figs. 1B-F; 2A-E; 3E, F). Inhibition of *Tgf-β1* and *Fn* by SP600125 might also play important roles in SP600125's protection against DN. However, this hypothesis needs to be further tested by manipulating *Tgf-β1* and *Fn* expression in the presence of SP600125 in

358 experimental models of DN. One possibility might be that NRF2, TGF-β1 and FN all
359 play pivotal roles, with crosstalk existing among them, functioning at different steps
360 as a circuit or a cascade. Supporting this view, higher expression of *Tgf-β1* and *Fn*
361 was found in the kidneys of the *Nrf2* KO diabetic mice, as compared with the WT
362 diabetic mice (Jiang et al. 2010; Wu et al. 2016). This indicates that NRF2 negatively
363 regulates *Tgf-β1* and *Fn* expression. Thus, upon diabetes, in addition to the
364 JNK-induced AP-1 transcriptional activity, JNK might enhance *Tgf-β1* and *Fn*
365 expression via inhibition of NRF2. The correlation between NRF2, TGF-β1 and FN in
366 DN needs to be further researched in future studies. In addition to the potential NRF2/
367 TGF-β1/FN network, other mechanisms, such as anti-inflammation (Pan et al. 2013)
368 and anti-renin-angiotensin system (Hong et al. 2016) may also contribute to
369 SP600125's protection. Notably, NRF2 activation by SP600125 might also account
370 for the anti-inflammatory function of SP600125, given that SP600125 completely lost
371 the ability to attenuate the pro-inflammatory factors TNF-α and VCAM-1 (Fig. 2D, E)
372 in the absence of NRF2. In the present study, a slight, but significant, decrease in
373 Masson's positive area (Fig. 1G, right panel) and CTGF protein (Fig. 2G, right panel)
374 was detected in the kidneys of the SP600125-treated *Nrf2* KO diabetic mice. These
375 observations suggest a NRF2-independent mechanism which plays a partial role in
376 SP600125's attenuation of diabetes-induced renal fibrosis, although the outcome of
377 this mechanism was minor compared to the potent effect of NRF2 (Figs. 1B-F; 2A-E).
378 Small molecules have been designed to disable KEAP1. Dimethyl fumarate,
379 bardoxolone methyl (Wang, et al. 2014) and sulforaphane (SFN) (Zhang and Hannink
380 2003) are the well-known small molecules that modify critical cysteines within
381 KEAP1 protein, leading to the release of NRF2 (Takaya, et al. 2012). Among these

KEAP1 inhibitors, dimethyl fumarate is currently in use for clinical treatment of multiple sclerosis (Gold, et al. 2012), demonstrating NRF2 as a viable drug target. Different from these KEAP1 inhibitors, SP600125 was found, in the present study, to decrease *Keap1* expression through inactivation of JNK, followed by NRF2 activation. The present study may suggest inhibition of *Keap1* expression as a strategy to activate NRF2, in addition to structural modification of the KEAP1 protein. In addition, the present study also suggests JNK gene silencing as an effective approach to activate NRF2 (Figs. 4E-H; 5A-E). Both SP600125 and JNK siRNA decreased the amount of p-JNK (Fig. 4E, right panel), which reflected an inhibited JNK activity. However, SP600125 and JNK siRNA were found, in the present study, to inactivate JNK through different mechanisms. Specifically, SP600125 inactivated JNK by inhibiting its phosphorylation (Fig. 4E, left panel), whereas JNK siRNA via decreasing the amount of JNK (Fig. 4E, middle panel).

Controversies exist within establishing the effect of MAPKs on the regulation of NRF2 signaling. It was assumed that activation of MAPKs may phosphorylate NRF2 at specific serine and threonine residues, thereby facilitating the release of NRF2 from KEAP1 (Lee and Surh 2005). However, opposed JNK activity and NRF2 expression were observed in experimental models of various diseases (Du, et al. 2016; Sahu, et al. 2015; Tan, et al. 2013; Ye, et al. 2015; Yenki, et al. 2013). Additionally, our previous report showed that inhibition of JNK by SP600125 or C66 led to NRF2 activation in the aortas of the diabetic mice (Liu et al. 2014). In line with these studies, the present study demonstrated a negative impact of JNK on NRF2 expression (Figs. 3B-G; 5A-E). Collectively, these findings shed light on diverse regulatory effects of JNK on NRF2. One possibility for the differential behaviors of

406 JNK could be the difference between disease conditions or cell types. A specific
407 effect of JNK may play a major role under a certain condition. The final outcome may
408 be the result of a combination of all the actions of JNK. In the present study,
409 enhancing *Keap1* expression was the most predominant action of JNK in inhibiting
410 NRF2. Although JNK-induced phosphorylation of NRF2 and adaptive response to the
411 oxidative stress might play positive roles in activating NRF2, these possible effects
412 could be minor, as compared with the effect of JNK on inducing *Keap1* expression.

413 In our previous study, SP600125 increased both *Nrf2* mRNA and protein in the
414 aorta (Liu et al. 2014). However, renal *Nrf2* mRNA was not altered by SP600125 in
415 the present study (Fig. 3A, left panel). This could be due to the variation of the JNK
416 function in different organs or cell types. Nonetheless, our previous study did show an
417 increased nuclear positive staining of NRF2 in the aorta (Liu et al. 2014), suggesting
418 an enhanced NRF2 nuclear translocation by SP600125. SP600125's negative effect
419 on *Keap1* expression has been further tested and verified in the present study (Fig.
420 4A, B, G, H). In our previous report, metallothionein (MT), a potent antioxidant, was
421 shown to be an important downstream target of NRF2 in DN (Wu et al. 2015), since
422 deletion of the *Mt* gene partially, but significantly, abolished the protective effects of
423 the NRF2 activator SFN. The rest of the protection produced by SFN in the absence
424 of MT might be due to the NRF2-induced activation of other canonical downstream
425 targets, such as *Ho1* and *Nqo1*.

426 It is noted that different stages of diabetic complications may have different
427 status of antioxidant defensive function. *Nrf2* expression and function were
428 upregulated in the aorta (Liu et al. 2014), heart (Bai, et al. 2013) and kidney (Cui, et
429 al. 2012) of mice 3 months post diabetes onset, which was a relatively early stage of

diabetes in mice. The activation of NRF2 antioxidant system could be due to the compensatory response to the stimulation by diabetes-induced oxidative stress (Bai et al. 2013), the effect of which adaptively overcomes the diabetes-induced injury. However, after a long-term exposure to diabetes-induced oxidative damage, the NRF2 antioxidant system tends to lose this function. This is evidenced by the impaired *Nrf2* expression and function in the hearts and kidneys of diabetic mice, 6 months post the onset of diabetes (Bai et al. 2013; Wu et al. 2016). In fact, decreased *Nrf2* expression was also observed in the hearts of diabetic patients as a chronic complication of diabetes (Tan, et al. 2011). This could possibly be caused by the impaired compensatory function of the antioxidant defensive response after a long-term exposure to hyperglycemia. In the present study, enhanced JNK function and *Keap1* expression in the 6-month diabetic kidneys might account for the impaired NRF2 function. Further studies are needed to elucidate the mechanism for the impaired *Nrf2* expression and function at the late stage of diabetes. In the present study, although renal NRF2 signaling was decreased in the WT diabetic mice (Fig. 3B-F, left panels), the presence of the basal NRF2 did play a protective role in the prevention of DN, since the *Nrf2* KO diabetic mice developed more severe renal dysfunction (Fig. 1B) and pathological changes (Fig. 1C-G), as compared with the WT diabetic mice.

Taken together, the present study demonstrates, for the first time, that NRF2 plays a critical role in SP600126 prevention of DN. Other findings suggest JNK to be a negative regulator of NRF2 in DN, the effect of which may be mediated by JNK-induced *Keap1* expression. This study may provide a basis for understanding the effect of JNK in DN, and may indicate JNK inactivation, JNK gene silencing and inhibition of *Keap1* expression as potential strategies for prevention of DN.

5. Declaration of interest

None.

6. Funding

This work was supported in part by the National Natural Science Foundation of China (81600573 to H.W.), Norman Bethune Program of Jilin University (2015438 to H.W.), Department of Science and Technology of Jilin Province (20170204032YY to J.W.), Development and Reform Commission of Jilin Province (2014G072 to J.W.), and Research Program of Jilin University (3R2173203428 to Y.J.).

7. Author contributions

H.W. conceived the project. H.W., J.W. and H.Z. designed the research. H.Z., X.L., S.Z., Y.J., Y.L. and Y.S. researched the data. H.W., J.W. and H.Z. wrote the manuscript. J.W., H.W., Y.J., H.Z., X.L., S.Z., Y.L. and Y.S. stimulated discussion. H.Z., X.L., S.Z., Y.J., Y.L., Y.S., J.W. and H.W. reviewed and revised the manuscript. H.W., J.W. and Y.J. provided funding. All the authors approved the version to be published.

References

Bai Y, Cui W, Xin Y, Miao X, Barati MT, Zhang C, Chen Q, Tan Y, Cui T, Zheng Y, et al. 2013 Prevention by sulforaphane of diabetic cardiomyopathy is associated with up-regulation of Nrf2 expression and transcription activation. *J Mol Cell Cardiol* **57** 82-95.

Bogoyevitch MA, Boehm I, Oakley A, Ketterman AJ & Barr RK 2004 Targeting the JNK MAPK cascade for inhibition: basic science and therapeutic potential. *Biochim Biophys Acta* **1697** 89-101.

Cai L, Wang J, Li Y, Sun X, Wang L, Zhou Z & Kang YJ 2005 Inhibition of superoxide generation and associated nitrosative damage is involved in metallothionein prevention of diabetic cardiomyopathy. *Diabetes* **54** 1829-1837.

Cui W, Bai Y, Miao X, Luo P, Chen Q, Tan Y, Rane MJ, Miao L & Cai L 2012 Prevention of diabetic nephropathy by sulforaphane: possible role of Nrf2 upregulation and activation. *Oxid Med Cell Longev* **2012** 821936.

Davis RJ 2000 Signal transduction by the JNK group of MAP kinases. *Cell* **103** 239-252.

De Borst MH, Prakash J, Melenhorst WB, van den Heuvel MC, Kok RJ, Navis G & van Goor H 2007 Glomerular and tubular induction of the transcription factor c-Jun in human renal disease. *J Pathol* **213** 219-228.

Dong W, Jia Y, Liu X, Zhang H, Li T, Huang W, Chen X, Wang F, Sun W & Wu H 2017 Sodium butyrate activates NRF2 to ameliorate diabetic nephropathy possibly via inhibition of HDAC. *J Endocrinol* **232** 71-83.

Dronavalli S, Duka I & Bakris GL 2008 The pathogenesis of diabetic nephropathy. *Nat Clin Pract Endocrinol Metab* **4** 444-452.

Du J, Zhang M, Lu J, Zhang X, Xiong Q, Xu Y, Bao Y & Jia W 2016 Osteocalcin improves nonalcoholic fatty liver disease in mice through activation of Nrf2 and inhibition of JNK. *Endocrine* **53** 701-709.

Gao P, Wei Y, Zhang Z, Zeng W, Sun D, Liu D, Hou B, Zhang C, Zhang N, Li H, et al. 2016 Synergistic effects of c-Jun and SP1 in the promotion of TGFbeta1-mediated diabetic nephropathy progression. *Exp Mol Pathol* **100** 441-450.

Gold R, Kappos L, Arnold DL, Bar-Or A, Giovannoni G, Selmaj K, Tornatore C, Sweetser MT, Yang M, Sheikh SI, et al. 2012 Placebo-controlled phase 3 study of oral BG-12 for relapsing multiple sclerosis. *N Engl J Med* **367** 1098-1107.

Ho C, Lee PH, Huang WJ, Hsu YC, Lin CL & Wang JY 2007 Methylglyoxal-induced fibronectin gene expression through Ras-mediated NADPH oxidase activation in renal mesangial cells. *Nephrology (Carlton)* **12** 348-356.

Hong Z, Hong Z, Wu D & Nie H 2016 Specific MAPK inhibitors prevent hyperglycemia-induced renal diseases in type 1 diabetic mouse model. *Mol Cell Biochem* **419** 1-9.

Jiang T, Huang Z, Lin Y, Zhang Z, Fang D & Zhang DD 2010 The protective role of Nrf2 in streptozotocin-induced diabetic nephropathy. *Diabetes* **59** 850-860.

Kensler TW, Wakabayashi N & Biswal S 2007 Cell survival responses to environmental stresses via the Keap1-Nrf2-ARE pathway. *Annu Rev Pharmacol Toxicol* **47** 89-116.

Lan T, Wu T, Gou H, Zhang Q, Li J, Qi C, He X, Wu P & Wang L 2013 Andrographolide suppresses high glucose-induced fibronectin expression in mesangial cells via inhibiting the AP-1 pathway. *J Cell Biochem* **114** 2562-2568.

Lee JS & Surh YJ 2005 Nrf2 as a novel molecular target for chemoprevention. *Cancer Lett* **224** 171-184.

Liu Y, Wang Y, Miao X, Zhou S, Tan Y, Liang G, Zheng Y, Liu Q, Sun J & Cai L 2014 Inhibition of JNK by compound C66 prevents pathological changes of the aorta in STZ-induced diabetes. *J Cell Mol Med* **18** 1203-1212.

Pan Y, Wang Y, Zhao Y, Peng K, Li W, Wang Y, Zhang J, Zhou S, Liu Q, Li X, et al. 2014 Inhibition of JNK Phosphorylation by a Novel Curcumin Analog Prevents High Glucose-Induced Inflammation and Apoptosis in Cardiomyocytes and the Development of Diabetic Cardiomyopathy. *Diabetes* **63** 3497-3511.

Pan Y, Zhang X, Wang Y, Cai L, Ren L, Tang L, Wang J, Zhao Y, Wang Y, Liu Q, et al. 2013 Targeting JNK by a new curcumin analog to inhibit NF-kB-mediated expression of cell adhesion molecules attenuates renal macrophage infiltration and injury in diabetic mice. *PLoS One* **8** e79084.

Ruiz S, Pergola PE, Zager RA & Vaziri ND 2013 Targeting the transcription factor Nrf2 to ameliorate oxidative stress and inflammation in chronic kidney disease. *Kidney Int* **83** 1029-1041.

Sahu BD, Mahesh Kumar J & Sistla R 2015 Baicalein, a Bioflavonoid, Prevents Cisplatin-Induced Acute Kidney Injury by Up-Regulating Antioxidant Defenses and Down-Regulating the MAPKs and NF-kappaB Pathways. *PLoS One* **10** e0134139.

Schena FP & Gesualdo L 2005 Pathogenetic mechanisms of diabetic nephropathy. *J Am Soc Nephrol* **16 Suppl 1** S30-33.

547 Sun W, Liu X, Zhang H, Song Y, Li T, Liu X, Liu Y, Guo L, Wang F, Yang T, et al.
548 2017 Epigallocatechin Gallate Upregulates NRF2 to Prevent Diabetic
549 Nephropathy via Disabling KEAP1. *Free Radic Biol Med*.
550 Takaya K, Suzuki T, Motohashi H, Onodera K, Satomi S, Kensler TW & Yamamoto M
551 2012 Validation of the multiple sensor mechanism of the Keap1-Nrf2 system.
552 *Free Radic Biol Med* **53** 817-827.
553 Tan M, Ouyang Y, Jin M, Chen M, Liu P, Chao X, Chen Z, Chen X, Ramassamy C,
554 Gao Y, et al. 2013 Downregulation of Nrf2/HO-1 pathway and activation of
555 JNK/c-Jun pathway are involved in Homocysteic acid-induced cytotoxicity in
556 HT-22 cells. *Toxicol Lett*.
557 Tan Y, Ichikawa T, Li J, Si Q, Yang H, Chen X, Goldblatt CS, Meyer CJ, Li X, Cai L,
558 et al. 2011 Diabetic downregulation of Nrf2 activity via ERK contributes to
559 oxidative stress-induced insulin resistance in cardiac cells in vitro and in vivo.
560 *Diabetes* **60** 625-633.
561 Wang Y, Feng W, Xue W, Tan Y, Hein DW, Li XK & Cai L 2009 Inactivation of
562 GSK-3beta by metallothionein prevents diabetes-related changes in cardiac
563 energy metabolism, inflammation, nitrosative damage, and remodeling. *Diabetes*
564 **58** 1391-1402.
565 Wang Y, Wang Y, Luo M, Wu H, Kong L, Xin Y, Cui W, Zhao Y, Wang J, Liang G, et
566 al. 2015 Novel curcumin analog C66 prevents diabetic nephropathy via JNK
567 pathway with the involvement of p300/CBP-mediated histone acetylation.
568 *Biochim Biophys Acta* **1852** 34-46.

569 Wang YY, Yang YX, Zhe H, He ZX & Zhou SF 2014 Bardoxolone methyl
570 (CDDO-Me) as a therapeutic agent: an update on its pharmacokinetic and
571 pharmacodynamic properties. *Drug Des Devel Ther* **8** 2075-2088.
572 Weigert C, Sauer U, Brodbeck K, Pfeiffer A, Haring HU & Schleicher ED 2000 AP-1
573 proteins mediate hyperglycemia-induced activation of the human TGF-beta1
574 promoter in mesangial cells. *J Am Soc Nephrol* **11** 2007-2016.
575 Wu H, Kong L, Cheng Y, Zhang Z, Wang Y, Luo M, Tan Y, Chen X, Miao L & Cai L
576 2015 Metallothionein plays a prominent role in the prevention of diabetic
577 nephropathy by sulforaphane via up-regulation of Nrf2. *Free Radic Biol Med* **89**
578 431-442.
579 Wu H, Kong L, Tan Y, Epstein PN, Zeng J, Gu J, Liang G, Kong M, Chen X, Miao L, et
580 al. 2016 C66 ameliorates diabetic nephropathy in mice by both upregulating
581 NRF2 function via increase in miR-200a and inhibiting miR-21. *Diabetologia* **59**
582 1558-1568.
583 Wu H, Zhou S, Kong L, Chen J, Feng W, Cai J, Miao L & Tan Y 2014a
584 Metallothionein deletion exacerbates intermittent hypoxia-induced renal injury in
585 mice. *Toxicol Lett* **232** 340-348.
586 Ye T, Zhen J, Du Y, Zhou JK, Peng A, Vaziri ND, Mohan C, Xu Y & Zhou XJ 2015
587 Green tea polyphenol (-)-epigallocatechin-3-gallate restores Nrf2 activity and
588 ameliorates crescentic glomerulonephritis. *PLoS One* **10** e0119543.
589 Yenki P, Khodagholi F & Shaerzadeh F 2013 Inhibition of phosphorylation of JNK
590 suppresses Abeta-induced ER stress and upregulates prosurvival mitochondrial
591 proteins in rat hippocampus. *J Mol Neurosci* **49** 262-269.

592 Zhang DD & Hannink M 2003 Distinct cysteine residues in Keap1 are required for
593 Keap1-dependent ubiquitination of Nrf2 and for stabilization of Nrf2 by
594 chemopreventive agents and oxidative stress. *Mol Cell Biol* **23** 8137-8151.
595 Zheng H, Whitman SA, Wu W, Wondrak GT, Wong PK, Fang D & Zhang DD 2011
596 Therapeutic potential of Nrf2 activators in streptozotocin-induced diabetic
597 nephropathy. *Diabetes* **60** 3055-3066.
598 Zhou X, Feng Y, Zhan Z & Chen J 2014 Hydrogen sulfide alleviates diabetic
599 nephropathy in a streptozotocin-induced diabetic rat model. *J Biol Chem* **289**
600 28827-28834.

601

602

603

604

605

606

607

608

609

610

611

612

Figure legends

Fig. 1. Deletion of the *Nrf2* gene led to a complete abolishment of SP600125's protection against diabetes-induced albuminuria and renal pathological change. Eight-week-old C57BL/6 WT and *Nrf2* KO male mice were induced to diabetes by streptozotocin. (**A**) Blood glucose levels were determined every four weeks post diabetes onset. Urinary albumin and creatinine were recorded at 24 weeks post diabetes onset with (**B**) UACR calculated. To evaluate renal pathological change, (**C**) PAS and (**D**) Masson's trichrome staining were performed, with (**E**) glomerular area and (**F**) mesangial matrix expansion quantified from PAS staining and (**G**) Masson's positive area quantified from Masson's trichrome staining. For (**E-G**), the data is normalized to WT Ctrl. All the data is presented as means ± SD (n = 8). *, $p < 0.05$ vs WT Ctrl; †, $p < 0.05$ vs KO Ctrl; ‡, $p < 0.05$ vs WT DM; §, $p < 0.05$ vs KO DM. Bar = 50 μm. Scatter plots: solid up triangle, WT Ctrl; solid down triangle, WT Ctrl/JNKi; solid left triangle, WT DM; solid right triangle, WT DM/JNKi; hollow up triangle, KO Ctrl; hollow down triangle, KO Ctrl/JNKi; hollow left triangle, KO DM; hollow right triangle, KO DM/JNKi. Bars: white, Ctrl; light grey, Ctrl/JNKi; dark grey, DM; black, DM/JNKi. Abbreviations: Ctrl, control; DM, diabetes mellitus; JNKi, the JNK inhibitor SP600125; KO, knockout; PAS, Periodic acid-Schiff; UACR, urinary albumin to creatinine ratio; WT, wild type.

Fig. 2. NRF2 was required for SP600125's alleviation of the diabetes-induced renal oxidative stress, inflammation and fibrosis. To further test the role of NRF2 in SP600125's protection against diabetes-induced renal injury, IHC staining was performed to assess renal expression of (**A**) 3-NT, an indicator of nitrosative damage.

Further, renal (**B**) MDA levels were measured by an MDA assay kit and protein levels of (**C**) iNOS, (**D**) TNF-α, (**E**) VCAM-1, (**F**) TGF-β1 and (**G**) CTGF were determined by Western blot. For (**B**), the data is normalized to WT Ctrl. For (**C-G**), the date is normalized to either WT Ctrl or KO Ctrl, respectively. All the data is presented as means ± SD (n = 8). *, $p < 0.05$ vs WT Ctrl; †, $p < 0.05$ vs KO Ctrl; ‡, $p < 0.05$ vs WT DM; §, $p < 0.05$ vs KO DM. Bars: white, Ctrl; light grey, Ctrl/JNKi; dark grey, DM; black, DM/JNKi. Abbreviations: 3-NT, 3-nitrotyrosine; CTGF, connective tissue growth factor; IHC, inmmunohistochemical; iNOS, inducible nitric oxide synthase; MDA, malondialdehyde; TGF-β1, transforming growth factor beta 1; TNF-α, tumor necrosis factor alpha; VCAM-1, vascular cell adhesion molecule 1. Other abbreviations are the same as those in Fig. 1.

Fig. 3. SP600125 preserved renal NRF2 protein and facilitated NRF2 nuclear translocation and function, without altering *Nrf2* mRNA. To test the effect of SP600125 on *Nrf2* gene expression and function, (**A**) *Nrf2* mRNA, protein levels of (**B**) t-NRF2 and (**C**) n-NRF2 were determined in both types of the mice. In order to evaluate NRF2 nuclear translocation, (**D**) ratio of n-NRF2/Histione H3 to t-NRF2/GAPDH was calculated. Further, NRF2 function was evaluated by determining the mRNA expression of (**E**) *Ho1* and (**F**) *Nqo1*. IHC staining of (**G**) HO1 and (**H**) NQO1 was further performed to assess the status of renal antioxidant activity. The data is normalized to WT Ctrl and presented as means ± SD (n = 8). *, $p < 0.05$ vs WT Ctrl; †, $p < 0.05$ vs WT DM. Bars: white, Ctrl; light grey, Ctrl/JNKi; dark grey, DM; black, DM/JNKi. Abbreviations: *Ho1*, heme oxygenase 1; n-NRF2, nuclear

NRF2; *Nqo1*, NAD(P)H dehydrogenase (quinone) 1; t-NRF2, total cellular NRF2. Other abbreviations are the same as those in Figs. 1, 2.

Fig. 4. SP600125 decreased *Keap1* expression through inhibition of JNK activity. With the aim of exploring the mechanism by which SP600125 activates NRF2, *Keap1* (**A**) mRNA and (**B**) protein, as well as ratios of (**C**) p-JNK to t-JNK and (**D**) p-c-Jun to t-c-jun were determined in the kidneys of the WT and *Nrf2* KO mice. To further define the effect of JNK inhibition on *Keap1* expression, MMCs were treated with HG, in the presence of either SP600125 or JNK siRNA, with ratios of (**E**) p-JNK to t-JNK and (**F**) p-c-Jun to t-c-jun, as well as *Keap1* (**G**) mRNA and (**H**) protein determined. For (**A-D**), the data is normalized to respective Ctrls and presented as means ± SD (n = 8). *, $p < 0.05$ vs WT Ctrl; †, $p < 0.05$ vs KO Ctrl; ‡, $p < 0.05$ vs WT DM; §, $p < 0.05$ vs KO DM. Bars: white, Ctrl; light grey, Ctrl/JNKi; dark grey, DM; black, DM/JNKi. For (**E-H**), the data is normalized to HG and presented as means ± SD (n = 3). *, $p < 0.05$ vs HG; †, $p < 0.05$ vs HG/NC. Bars: white, HG; light grey, HG/JNKi; dark grey, HG/RFect^{PM}; black, HG/NC; white with stripes, HG/siJNK; Abbreviations: HG, high glucose; *Keap1*, Kelch-like ECH-associated protein 1; NC, negative control siRNA; p-c-Jun, phosphorylated c-Jun; p-JNK, phosphorylated JNK; RFect^{PM}, the transfection reagent; siJNK, JNK siRNA; t-c-Jun, total c-Jun; t-JNK, total JNK. Other abbreviations are the same as those in Fig. 1.

Fig. 5. Both SP600125 and JNK siRNA preserved NRF2 protein and enhanced its nuclear translocation and function. In order to test the effect of JNK inhibition on NRF2 expression and function, MMCs were subjected to HG, in the presence of

either SP600125 or JNK siRNA. (**A**) t-NRF2 and (**B**) n-NRF2 levels were determined by Western blot. (**C**) n-NRF2/Histione H3 to t-NRF2/GAPDH was calculated to reflect NRF2 nuclear translocation. mRNA levels of (**D**) *Ho1* and (**E**) *Nqo1* were determined by RT-PCR. The data is normalized to HG and presented as means ± SD (n = 3). *, $p < 0.05$ vs HG; †, $p < 0.05$ vs HG/NC. Bars: white, HG; light grey, HG/JNKi; dark grey, HG/ RFect^{PM}; black, HG/NC; white with stripes, HG/siJNK; Abbreviations are the same as those in Figs. 3, 4.

Fig. 6. JNK inhibition by either SP600125 or JNK siRNA decreased oxidative damage and expression of inflammatory and fibrotic genes in HG-treated MMCs. SP600125 and JNK siRNA were further tested for their roles in alleviating HG-induced oxidative stress, inflammation and fibrosis in MMCs. (**A**) MDA levels and mRNA expression of (**B**) *iNos*, (**C**) *Vcam-1*, (**D**) *Icam-1*, (**E**) *Fn* and (**F**) *Col4* were determined. The data is normalized to HG and presented as means ± SD (n = 3). *, $p < 0.05$ vs HG; †, $p < 0.05$ vs HG/NC. Bars: white, HG; light grey, HG/JNKi; dark grey, HG/ RFect^{PM}; black, HG/NC; white with stripes, HG/siJNK; Abbreviations: *Col4*, collagen 4; *Fn*, fibronectin. Other abbreviations are the same as those in Figs. 2, 4.

Fig. 1

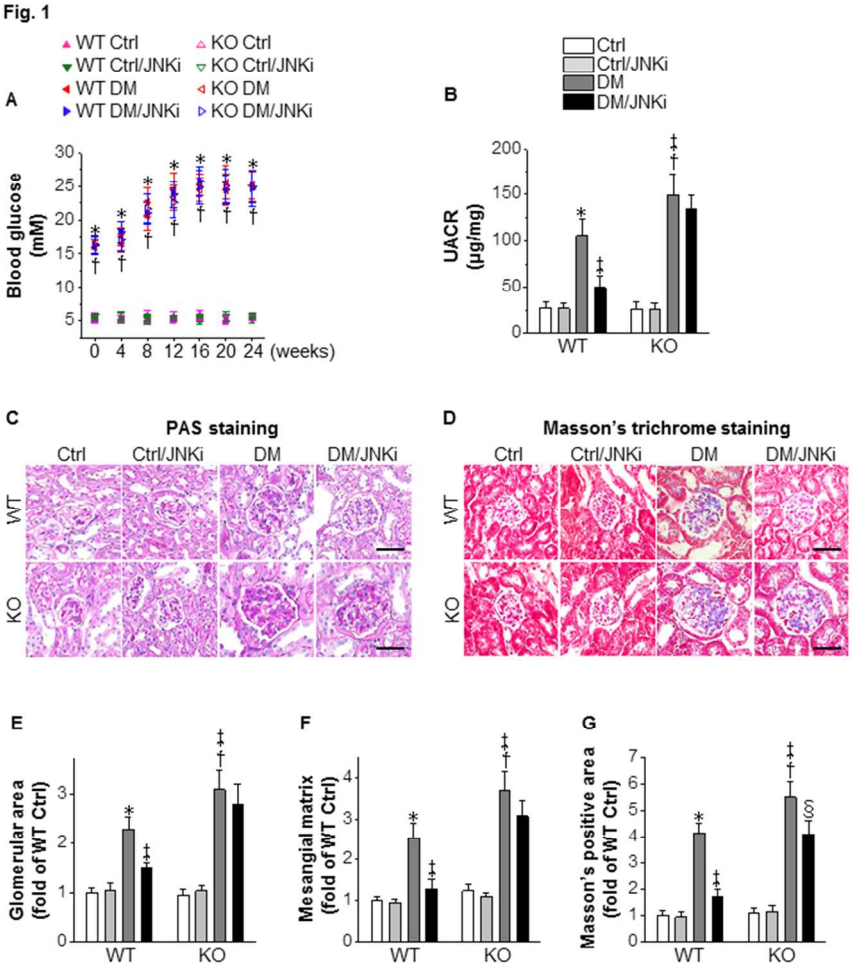

190x254mm (96 x 96 DPI)

Fig. 2

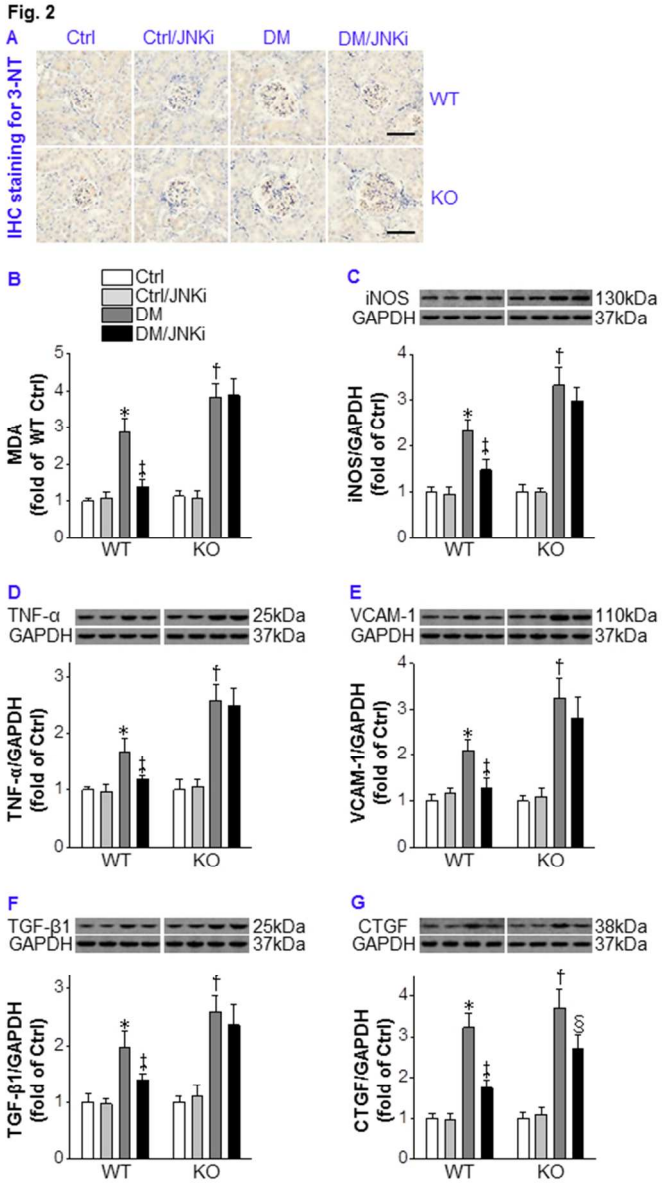

190x254mm (96 x 96 DPI)

Fig. 3

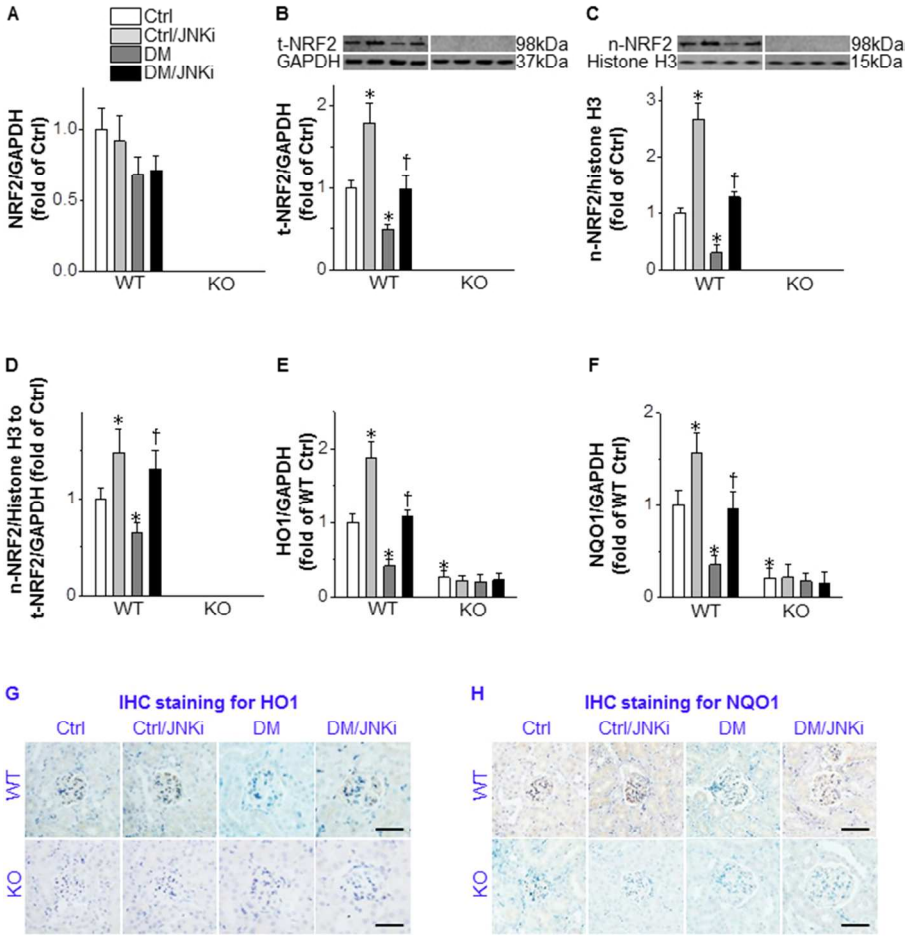

190x254mm (96 x 96 DPI)

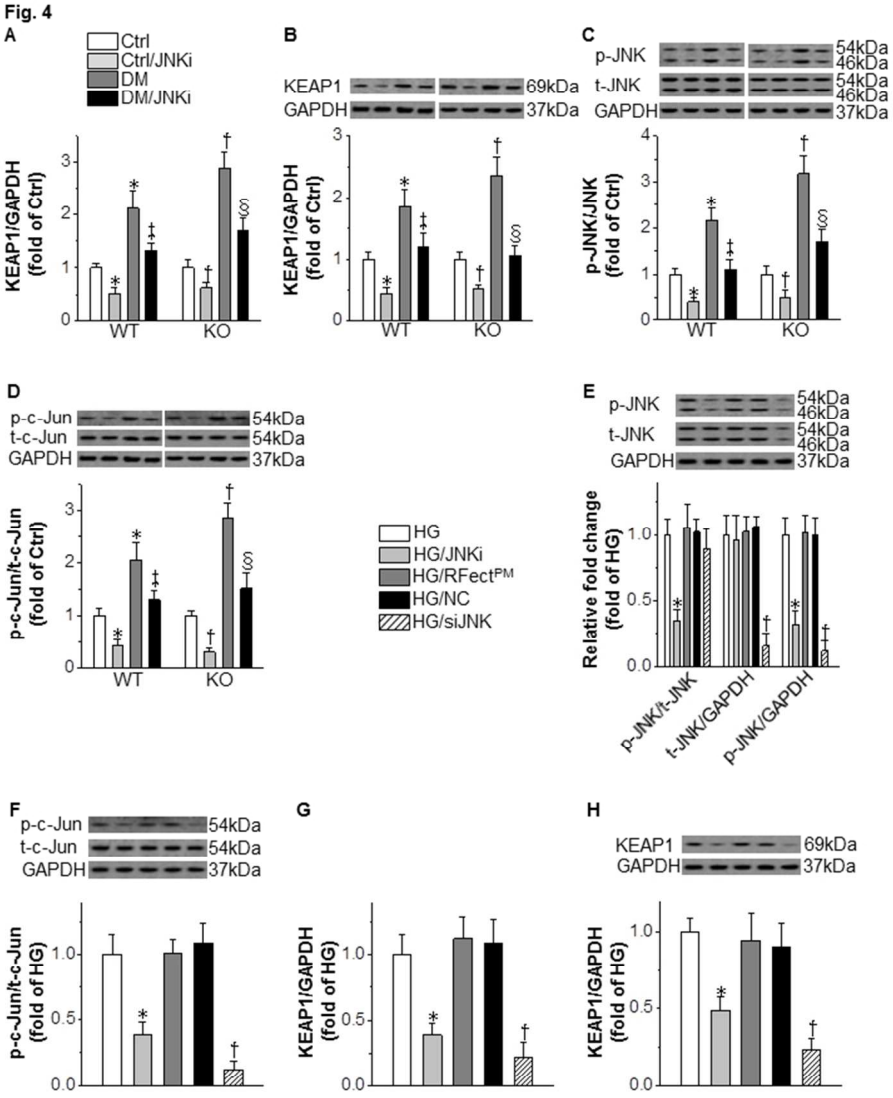

190x254mm (96 x 96 DPI)

Fig. 5

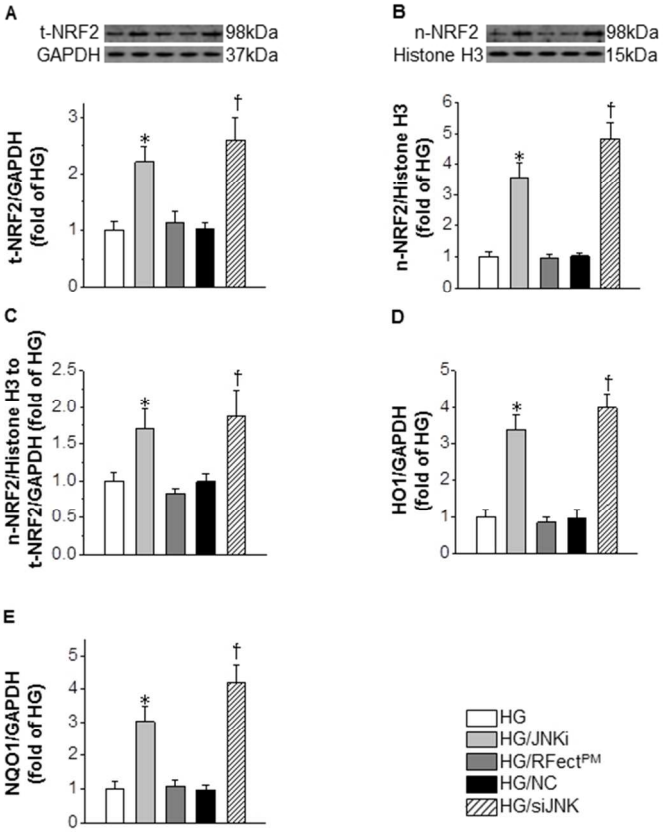

190x254mm (96 x 96 DPI)

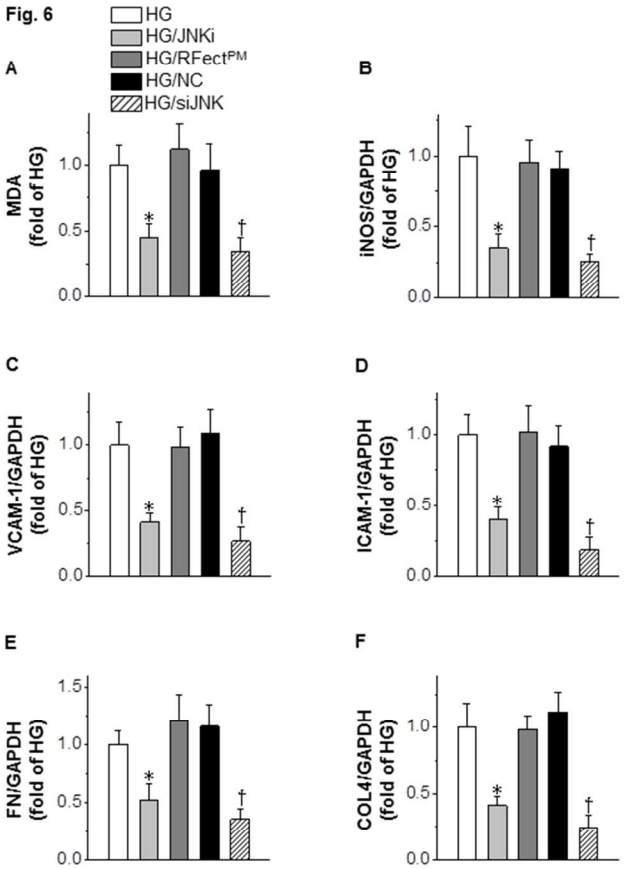

190x254mm (96 x 96 DPI)